



Research article

Taste receptor type 1 member 3 is required for the fertility of male mice

Woo-Jeong Shon^{a,b,1,*}, Hobin Seong^{b,1}, Jae Won Song^{b,1}, Dong-Mi Shin^{a,b}^a Research Institute of Human Ecology, Seoul National University, Gwanak-gu, Seoul 08826, Republic of Korea^b Department of Food and Nutrition, Seoul National University College of Human Ecology, Gwanak-gu, Seoul 08826, Republic of Korea

ARTICLE INFO

Keywords:

Leydig cell
Male infertility
PKA/CREB/STAR signaling
Taste receptor type 1 member 3
Testosterone

ABSTRACT

Male infertility is a global health concern. However, its underlying pathophysiology remains unclear. Taste receptor type 1 member 3 (TAS1R3) is highly expressed in the testes, indicating its potential involvement in male fertility. Using wild-type and *Tas1r3* knockout (KO) mice, we investigated whether TAS1R3 modulates male reproductive function. *Tas1r3* KO mice exhibited reduced male fertility compared to WT mice, with fewer live pups per litter and a delayed first litter. Testicular transcriptome analysis indicated suppressed PKA/CREB/STAR signaling-mediated testosterone synthesis in *Tas1r3* KO mice. *In silico* single-cell RNA sequencing revealed considerably higher *Tas1r3* expression in Leydig cells than in other testicular cell subtypes. An *in vitro* study validated that *Tas1r3* knockdown downregulated the expression of *Creb1* and steroidogenic genes in Leydig cells. Our results suggest that testicular TAS1R3 is intricately involved in male reproduction via the PKA/CREB/STAR signaling pathway, highlighting its potential as a promising target for addressing male infertility.

1. Introduction

Infertility, characterized by the failure to achieve conception following one year of consistent and unprotected sexual intercourse, has emerged as a pervasive global health concern, impacting 48 million couples [1,2]. Infertility experienced by approximately 50 % of couples can be partly or wholly attributed to male factor [3,4]. The common characteristics of male infertility include a decline in sperm count (azoospermia or oligozoospermia) [5], reduced sperm motility (asthenozoospermia) [6], or an increased number of morphologically abnormal sperms (teratozoospermia) [7]. Recent studies have highlighted the concerns regarding the global downward trends in sperm quality and the rising prevalence of male infertility [8,9]. The decline in male fertility must be navigated because infertility negatively affects human well-being and imposes a huge economic burden on the public health system and welfare and individuals experiencing infertility [10–12]. Although male infertility factors substantially contribute to human infertility, current studies on infertility have focused more on females than on males [13].

Testosterone, synthesized by Leydig cells in the testes, is an essential hormone needed for the development of male characteristics and the process of sperm production [14]. In mammals, there are two distinct types of Leydig cells, namely fetal Leydig cells (FLCs) and adult Leydig cells (ALCs), which undergo sequential development in the fetal and adult testes, respectively [15]. However, during the process of sexual maturation, notably during puberty, FLCs are replaced by ALCs, which have the responsibility of sustaining

* Corresponding author. Research Institute of Human Ecology, Seoul National University, Gwanak-gu, Seoul 08826, Republic of Korea.

E-mail address: wjson@snu.ac.kr (W.-J. Shon).¹ These authors equally contributed to this manuscript.<https://doi.org/10.1016/j.heliyon.2024.e24577>

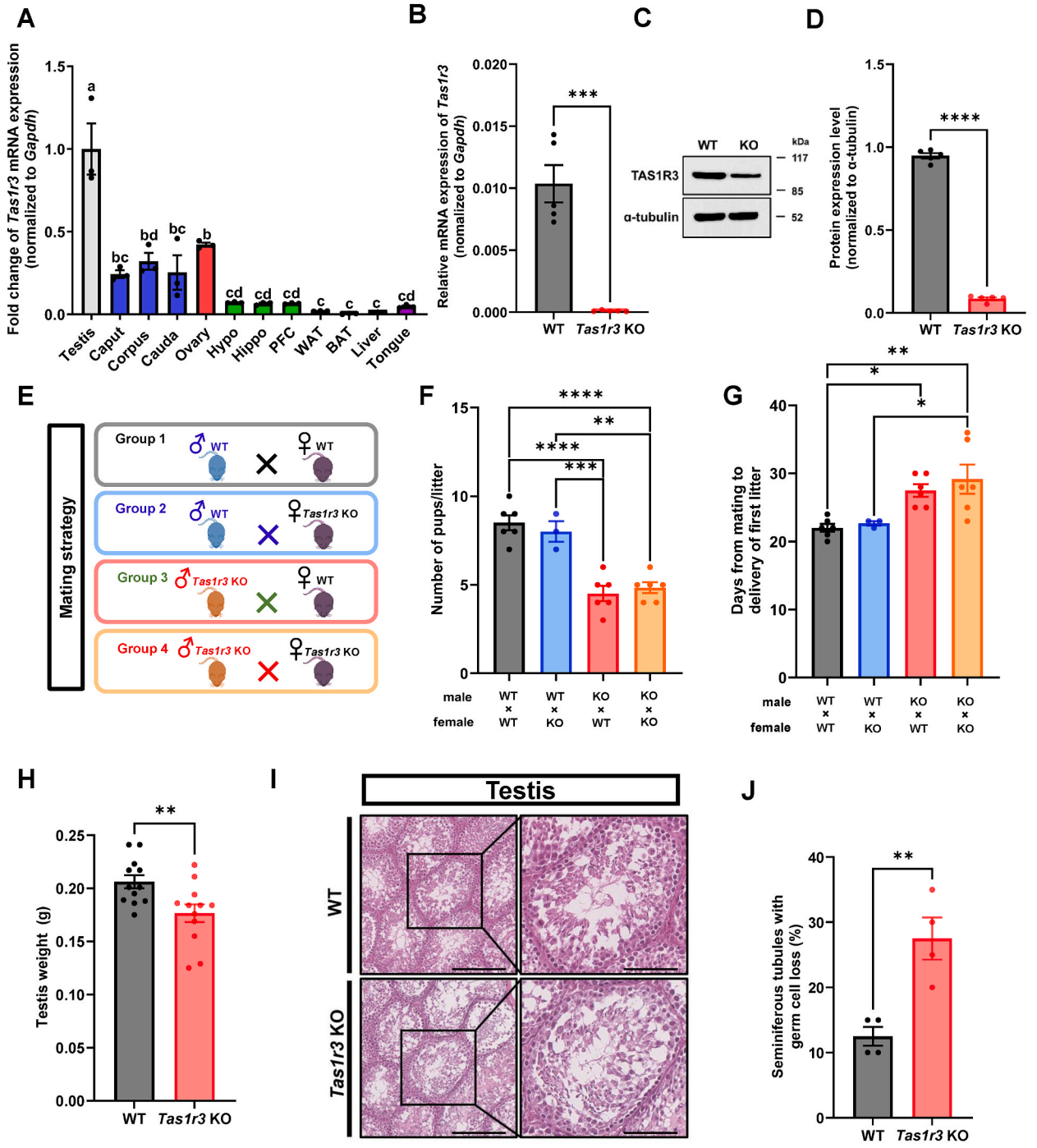
Received 20 September 2023; Received in revised form 28 December 2023; Accepted 10 January 2024

Available online 18 January 2024

2405-8440/© 2024 Published by Elsevier Ltd.

This is an open access article under the CC BY-NC-ND license

<http://creativecommons.org/licenses/by-nc-nd/4.0/>.



(caption on next page)

Fig. 1. *Tas1r3* deficiency causes severe reproductive defects in male mice. (A) The relative mRNA expression level of *Tas1r3* in male and female reproductive organs ($n = 3$ /tissue). (B) Comparison of *Tas1r3* expression in WT and *Tas1r3* KO mice at the transcript levels and (C–D) protein levels ($n = 5$ /group). (E) Schematic of the experimental plan. (F) Litter size produced by mating pairs of the shown genotypes of mice (male WT x female WT: $n = 6$, male WT x female *Tas1r3* KO: $n = 3$, male *Tas1r3* KO x female WT: $n = 6$, male *Tas1r3* KO x female *Tas1r3* KO: $n = 6$). (G) The number of days from mating to delivery of first litter (male WT x female WT: $n = 6$, male WT x female *Tas1r3* KO: $n = 3$, male *Tas1r3* KO x female WT: $n = 6$, male *Tas1r3* KO x female *Tas1r3* KO: $n = 6$). (H) Testicular weight (g) ($n = 12$ /group). (I) Representative hematoxylin and eosin-stained testis sections. Scale bars = 200 μm ($n = 4$ /group). (J) Percentage of tubules showing loss of germ cells ($n = 4$ /group). See Fig. S2 for uncropped gel images in Fig. 1C. All data are presented as mean \pm SEM. * = $P < 0.05$, ** = $P < 0.01$, *** = $P < 0.001$, and **** = $P < 0.0001$ (one-way ANOVA followed by Tukey's post-hoc test or unpaired Student's *t*-test). Different alphabets in the top of the bars indicate significant differences between groups (one-way ANOVA followed by Tukey's post-hoc test). ANOVA, analysis of variance; BAT, brown adipose tissue; Hippo, hippocampus; Hypo, hypothalamus; PFC, prefrontal cortex; KO, knockout; WAT, white adipose tissue; WT, wild-type. (For interpretation of the references to colour in this figure legend, the reader is referred to the Web version of this article.)

secondary sexual characteristics and supporting spermatogenesis by producing testosterone [16–18]. Although mature adults with low testosterone levels can produce sperms, testosterone has been linked to decreased sperm motility, which prevents sperms from moving through the vagina to the fallopian tubes to meet and fertilize the oocyte [19]. Men with asthenozoospermia, a condition defined by the World Health Organization as insufficient total sperm motility (below 40 %), exhibited significantly lower levels of testosterone compared to healthy normozoospermic men [20]. Thus, the key molecules regulating testosterone synthesis must be elucidated for infertility treatment.

Taste receptor type 1 member 3 (TAS1R3), responsible for mediating taste perception, is a G protein-coupled receptor (GPCR) expressed in gustatory cells located within the taste buds on the tongue [21]. TAS1R3 functions as a heterodimer to perceive umami (TAS1R1/TAS1R3) and sweet (TAS1R2/TAS1R3) taste in cells sensing amino acid, fructose, and glucose molecules [22]. Strikingly, TAS1R3 is expressed in extraoral tissues, including the ovaries, brain, adipocytes, and liver [23–26]. In particular, TAS1R3 is

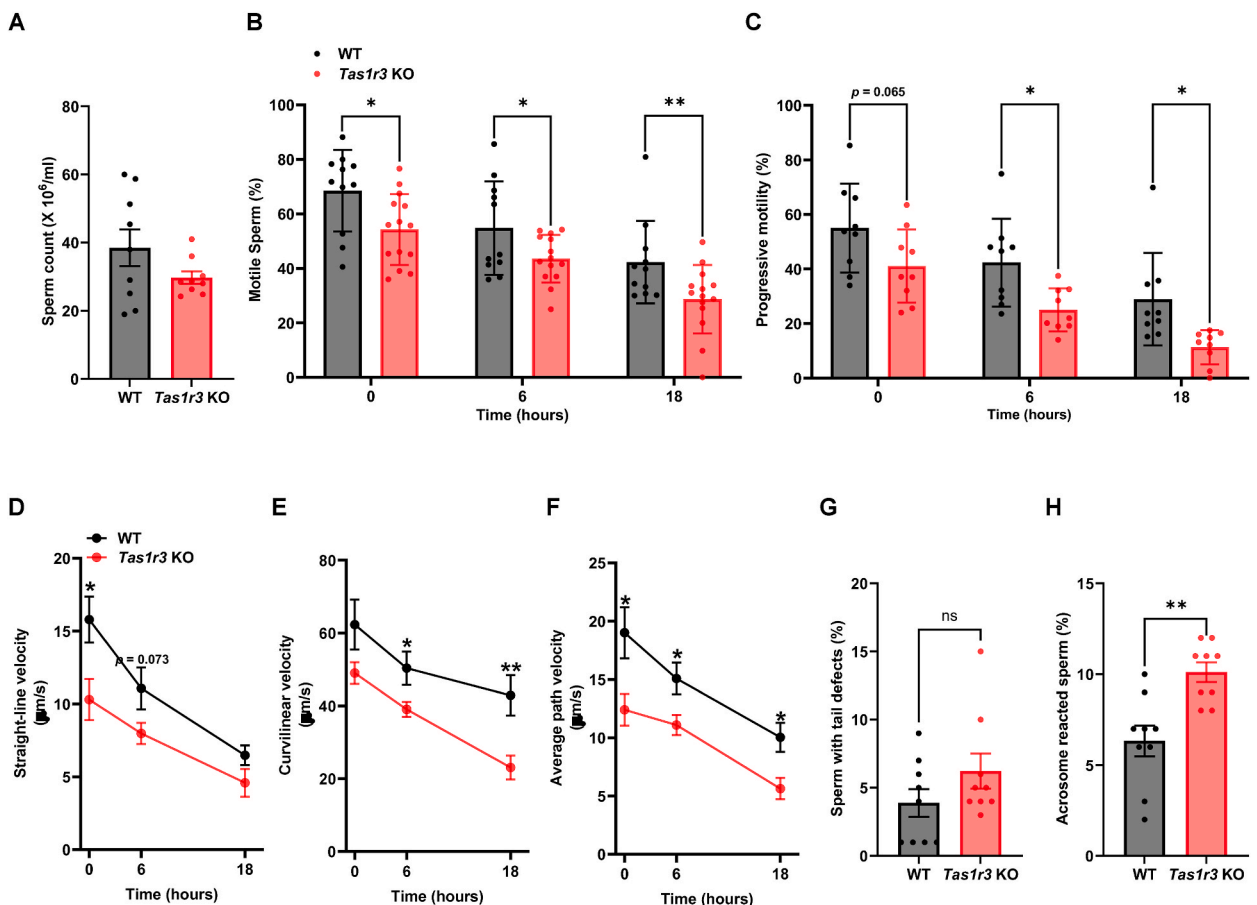


Fig. 2. Sperm quality is impaired in *Tas1r3* KO mice. (A) Sperm count ($n = 9$ /group). (B) Sperm motility and (C) progressive motility analyzed by CASA system ($n = 9$ /group). (D) Straight-line velocity, (E) curvilinear velocity, and (F) average path velocity ($n = 9$ /group). (G) Percentage of sperms with tail defects ($n = 9$ /group). (H) Percentage of acrosome-reacted sperms ($n = 9$ /group). All data are presented as mean \pm SEM. * = $P < 0.05$ and ** = $P < 0.01$ (unpaired Student's *t*-test). CASA, computer-assisted sperm analysis; KO, knockout; WT, wild-type.

abundantly expressed in testes [27], and previous studies have proposed an association between TAS1R3 and male fertility, suggesting that its expression in the testes is cell-specific and associated with spermatogenesis [28–30]. In addition, *Tas1r3* has been proposed to be involved in sperm chemotaxis [31]. Although these findings suggest that TAS1R3 may play a role in the regulation of male fertility, the precise molecular mechanism by which testicular TAS1R3 regulates male reproduction has not yet been studied. Therefore, we aimed to elucidate the molecular mechanism by which TAS1R3, highly expressed in the testes, regulates male fertility.

2. Results

2.1. *TAS1R3* deficiency induces impairment of male reproductive performance and abnormal testicular histology

To ascertain the relative expression of *Tas1r3* in various organs, quantitative real-time polymerase chain reaction (qRT-PCR) was performed to assess *Tas1r3* mRNA levels in various tissues from wild-type (WT) mice, including the testis; caput, corpus, and cauda of the epididymides; ovary; hypothalamus (Hypo); hippocampus (Hippo); prefrontal cortex (PFC); white adipose tissue (WAT); brown adipose tissue (BAT); liver; and tongue. *Tas1r3* was most highly expressed in the testes than in other organs (Fig. 1A).

The mouse model with genetic deletion of *Tas1r3* was developed to explore the involvement of TAS1R3 in male reproduction (Fig. 1B and C). To examine whether *Tas1r3* has a role in sustaining male fertility, WT and *Tas1r3* KO male mice were crossed with age-

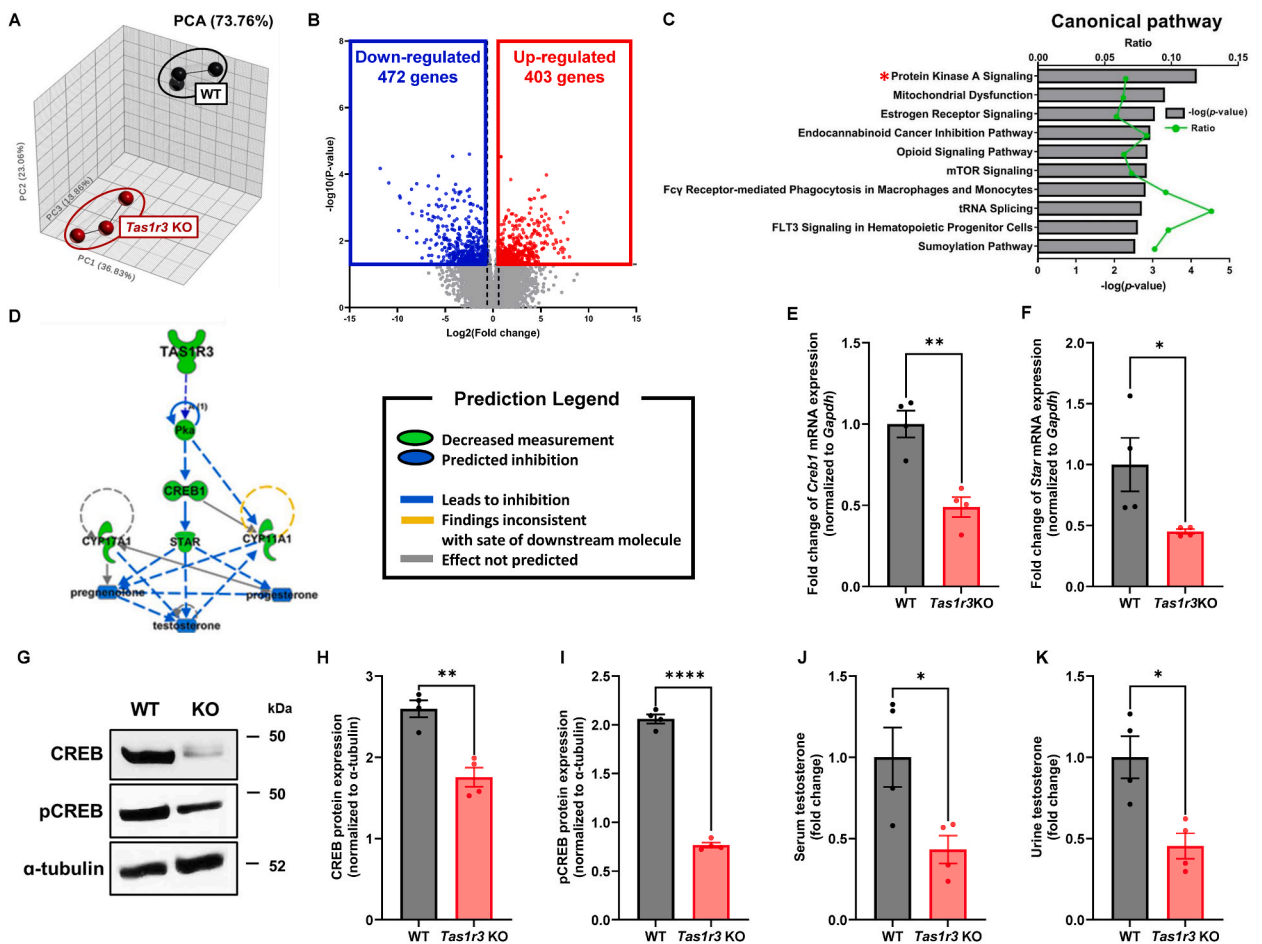


Fig. 3. Deficiency in *Tas1r3* significantly modifies the gene expression profiles of the testes. (A) Principal component analysis of the *Tas1r3* KO group versus WT group ($n = 3/\text{group}$). (B) Volcano plot of all DEGs between WT and the *Tas1r3* KO mice. Red dots indicate high relative expression of genes ($n = 403$), and blue dots indicate low relative expression of genes ($n = 472$). Unpaired two-tailed Student's *t*-test; thresholds of adjusted *P*-value < 0.05 and 1.5-fold change restriction analysis. (C) Canonical pathways significantly detected by IPA in *Tas1r3* KO mice compared to WT mice. (D) Gene interaction network map comprising the DEGs associated with the role of CREB in the testes. (E) *Creb1* and (F) *Star* mRNA expression levels ($n = 4/\text{group}$). (G) Representative Western blot of CREB and pCREB in the testes. (H) CREB and (I) pCREB protein expression levels ($n = 4/\text{group}$). Testosterone levels in (J) serum and (K) urine ($n = 4/\text{group}$). See Fig. S2 for uncropped gel images in Fig. 3G. All data are presented as mean \pm SEM. * = $P < 0.05$ and ** = $P < 0.01$ (unpaired Student's *t*-test). DEGs, differentially expressed genes; GSEA, gene set enrichment analysis; IPA, ingenuity pathway analysis; KO, knockout; PKA, protein kinas A; WT, wild-type. (For interpretation of the references to colour in this figure legend, the reader is referred to the Web version of this article.)

matched WT or *Tas1r3* KO female mice (Fig. 1D). Interestingly, regardless of female genotype, *Tas1r3* KO male mice exhibited a smaller litter size than WT male mice (Fig. 1E). Similarly, deficiency of *Tas1r3* in male mice resulted in a longer latency of delivery for the first litter compared to WT male mice. Meanwhile, *Tas1r3* deficiency did not result in a delayed latency in female mice, contrasting with *Tas1r3*-deficient male mice (Fig. 1F).

Because *Tas1r3* KO mice exhibited a significant reduction in testis weights compared to WT mice (Fig. 1G), histological analysis of testicular and epididymal tissues were conducted through hematoxylin and eosin (H&E) staining to assess the structural and physiological characteristics of male reproductive tissues. Although WT mice showed normal and healthy structures of the testicular seminiferous tubules, significantly damaged structures were observed in the seminiferous tubules of *Tas1r3* KO mice (Fig. 1H). Furthermore, the deficiency of *Tas1r3* resulted in a significantly higher percentage of loss of germ cells in seminiferous tubules compared to WT mice (Fig. 1I and J). Conversely, both *Tas1r3* KO and WT mice exhibited no remarkable differences in the epididymal sections (Figs. S1A and S1B).

These results suggest that TAS1R3 deficiency impairs male reproductive performance and testicular histological structures in mice.

2.2. *Tas1r3* KO mice exhibited deteriorated sperm quality

To explore the underlying causes driving the impaired reproductive performance in *Tas1r3* KO mice, we further assessed male reproductive function. We analyzed sperm count and viability and performed computer-assisted sperm analysis to examine general sperm quality using sperm suspensions collected from WT and *Tas1r3* KO mice.

The epididymal sperm count was lower in *Tas1r3* KO mice; however, the difference was not significant (Fig. 2A). The percentages of sperm with motility and progressive motility were measured at three time points: 0, 6, and 18 h after sperm collection. At all time points, sperms collected from *Tas1r3* KO mice showed deteriorated motility compared with those from WT mice (Fig. 2B). Furthermore, the progressive motility of sperms was decreased at 6 and 18 h in *Tas1r3* KO mice (Fig. 2C). In addition, kinematic values such as straight-line velocity (VSL), curvilinear velocity (VCL), and average path velocity (VAP) were assessed for sperm velocity assessment at the same time points. After 0 and 18 h, VSL was significantly reduced in sperm collected from *Tas1r3* KO mice (Fig. 2D). VCL and VAP were lowered in sperms collected from *Tas1r3* KO mice at all time points (Fig. 2E and F). Sperm motility defects are frequently linked to the formation and function of sperm tail structures [32]. Although not statistically significant, an observed tendency for elevated sperm tail abnormalities in *Tas1r3* KO mice was confirmed (Fig. 2G).

The proper regulation of the acrosome reaction (AR) is vital in preparing sperm for fertilization process, and unexpected spontaneous AR can occur because of sperm death or exposure to a stressor impacting the acrosome membrane [33,34]. In *Tas1r3* KO mice, the percentage of sperms with an AR was higher than WT mice, despite using non-capacitating media throughout the procedures and not administering AR-triggering stressors (Fig. 2H).

These results show that TAS1R3 deficiency leads to sperm quality impairment.

2.3. *Tas1r3* deficiency alters gene expression profiles in the testes

We performed RNA sequencing experiments on the testes to elucidate the underlying molecular mechanisms by which TAS1R3

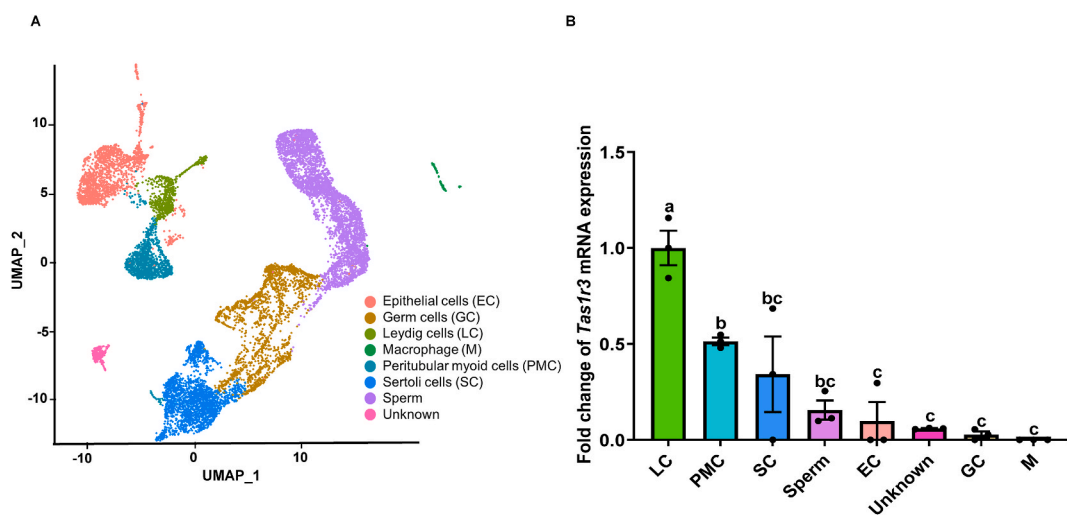


Fig. 4. *Tas1r3* is expressed at highest level in Leydig cells between cell types in the testes. (A) UMAP plot showing cell type clusters. (B) The relative mRNA expression level of *Tas1r3* across cell types ($n = 3/\text{cell type}$). All data are presented as mean \pm SEM. Different alphabets in the top of the bars indicate significant differences between cell types (one-way ANOVA followed by Tukey's post-hoc test). ANOVA, analysis of variance; EC, epithelial cell; GCs, germ cells; KO, knockout; LC, Leydig cell; M, macrophage; PMC, peritubular myoid cell; SC, Sertoli cell; scRNA-seq, single-cell RNA sequencing; UMAP, uniform manifold approximation and projection; WT, wild-type.

deficiency impairs male fertility. The testicular gene expression profiles between *Tas1r3* KO mice and WT mice were found to be significantly different through principal component analysis. (Fig. 3A). Assessment of differential expression [$|\text{fold change}| \geq 1.5$, adjusted P -value ≤ 0.05] revealed 875 differentially expressed genes (DEGs) between WT and *Tas1r3* KO mice; Upregulation of 403 genes and downregulation of 472 genes were observed in *Tas1r3* KO mice in comparison to WT mice. (Fig. 3B).

The extracted DEGs were subjected to a subsequent bioinformatics analysis to explore the fundamental molecular mechanism contributing to infertility in the context of *Tas1r3* deficiency.

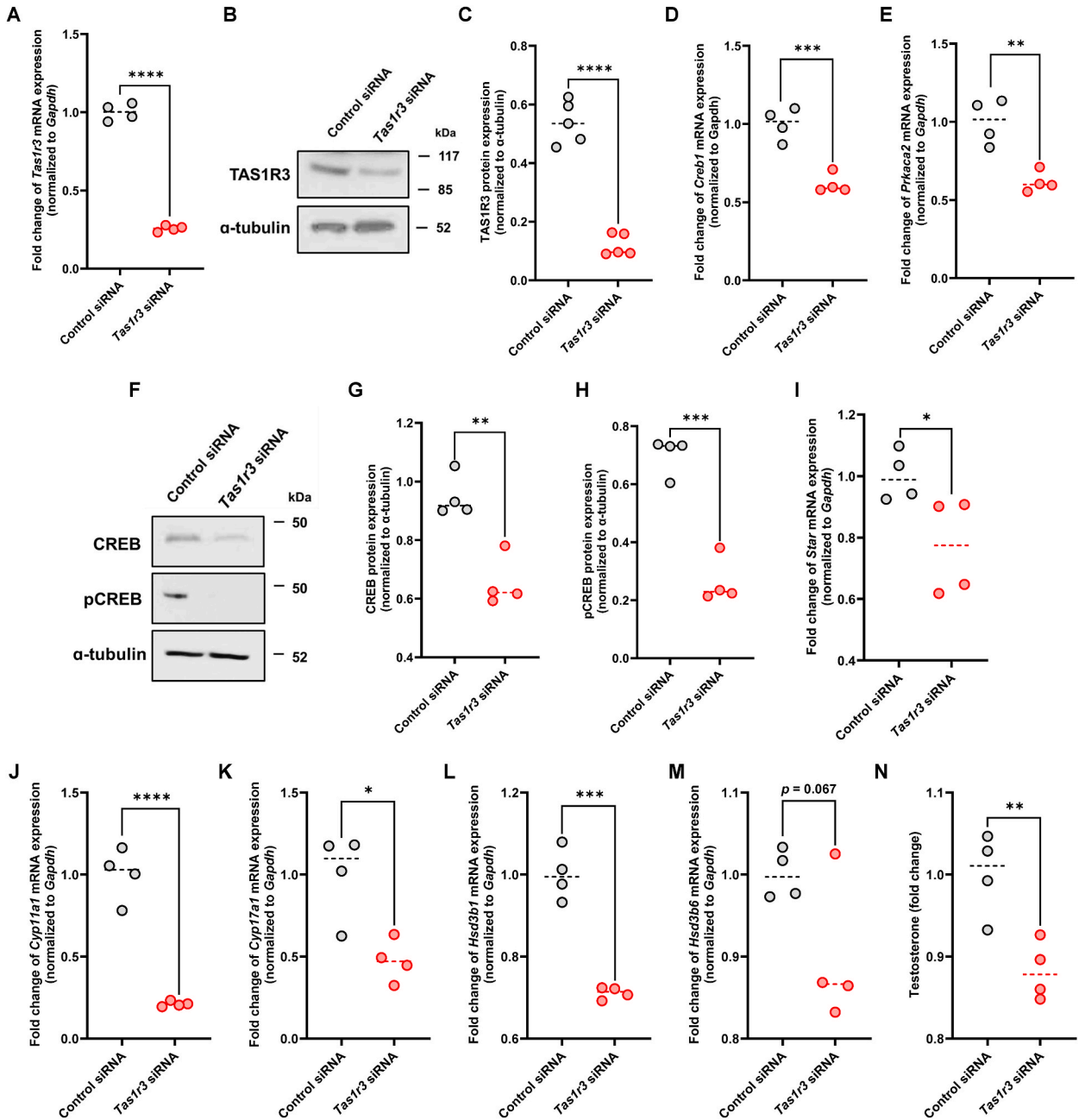


Fig. 5. *Tas1r3* knockdown suppresses PKA/CREB signaling-mediated testosterone synthesis in TM3 cells. Evaluation of siRNA-mediated *Tas1r3* suppression in cultured TM3 cells at the (A) mRNA ($n = 4/\text{group}$) and (B–C) protein levels ($n = 5/\text{group}$). Relative mRNA expression of (D) *Prkaca* and (E) *Creb1* genes in transfected TM3 cells ($n = 4/\text{group}$). (F) Representative Western blot of CREB and pCREB in TM cells. (G) Total CREB and (H) pCREB protein levels in transfected TM3 cells ($n = 4/\text{group}$). (E–M) Relative mRNA expression of steroidogenic genes, *Star*, *Cyp11a1*, *Cyp17a11*, *Hsd3b1*, and *Hsd3b6* in transfected TM3 cells ($n = 4/\text{group}$). (N) Analysis of testosterone concentrations in TM3 cell culture supernatants ($n = 4/\text{group}$). See Fig. S2 for uncropped gel images in Fig. 5B and F. All data are presented as mean \pm SEM. * = $P < 0.05$, ** = $P < 0.01$, *** = $P < 0.001$, and **** = $P < 0.0001$ (unpaired Student’s t -test).

Ingenuity Pathway Analysis (IPA) was utilized to identify the top significant canonical pathways. Protein kinase A (PKA) signaling ($P = 7.59E-05$) exhibited the most notable inhibition in *Tas1r3* KO mice when compared to WT mice (Fig. 3C).

In the IPA network analysis, it was predicted that CREB, regulated by the PKA signaling pathway, would be inhibited (Fig. 3D). In *Tas1r3* KO mice, we verified that the transcript levels of *Creb1* and its target *Star* were significantly lower than those in WT mice (Fig. 3E and F). Western blotting was performed to confirm whether alterations in the expression of *Creb1*, influenced by TAS1R3 deficiency, were mirrored at the protein level. Consistently, in *Tas1r3* KO mice, both CREB and phosphorylated CREB (pCREB) in the testes showed lower expressions than in WT mice (Fig. 3G–I). Furthermore, *Tas1r3* KO mice exhibited significantly lower serum and urinary testosterone levels compared to those in WT mice (Fig. 3J–K). These results highlight that PKA/CREB/STAR signaling related to testosterone synthesis is altered by *Tas1r3* deficiency.

2.4. *Tas1r3* is the most abundant in leydig cells among testicular cell subtypes

Because we used a conventional KO mouse model, we attempted to identify testicular cells that predominantly expressed *Tas1r3* to validate the direct effects of TAS1R3 on PKA/CREB/STAR signaling. We accessed a single-cell RNA sequencing dataset previously published in the Gene Expression Omnibus (GEO) database. After filtering low-quality cells, 12,675 cells were retained for downstream bioinformatics analyses. To visualize multidimensional data, we applied the uniform manifold approximation and projection (UMAP) technique and identified eight clusters corresponding to unique cell types (Fig. 4A). By analyzing gene expression across different cell types, we confirmed that *Tas1r3* exhibited the highest expression levels in Leydig cells compared with levels in other cell types within heterogeneous testicular tissues (Fig. 4B).

2.5. *Tas1r3* controls testosterone biosynthesis by regulating PKA/CREB signaling in leydig cells

To ascertain if TAS1R3 directly regulates the PKA/CREB axis in Leydig cells, we employed siRNA-mediated knockdown of *Tas1r3* in TM3 cells, a cell line derived from mouse Leydig cells that displayed high *Tas1r3* expression. At both the transcriptional and protein levels, the expression of TAS1R3 was significantly decreased following transfection with siRNA targeting *Tas1r3* (Fig. 5A–C). The expression levels of *Prkaca* and *Creb1* were significantly reduced by *Tas1r3* knockdown, resulting in a significant decrease in total CREB and pCREB (Fig. 5D–H). Consistent with the preceding animal experiments, we observed a significant impairment in the expression of *Star* following *Tas1r3* knockdown. Furthermore, steroidogenic genes essential for testosterone synthesis, including members of the cytochrome P450 families (*Cyp11a1* and *Cyp17a1*), as well as *Hsd3b1*, exhibited impaired expression following *Tas1r3* knockdown. Further, testosterone levels were significantly decreased by *Tas1r3* knockdown in TM3 cell culture supernatants (Fig. 5N).

3. Discussion

In this study, we hypothesized that TAS1R3, a taste receptor highly expressed in the testes, plays a role in the molecular mechanisms underlying male reproduction. *Tas1r3* deficiency downregulated the PKA signaling pathway in mouse testes, suppressing the transcription factor CREB and its target, STAR, and subsequently affecting testosterone levels. Leydig cells exhibited a higher expression of *Tas1r3* than any other cell types within the testes, as revealed by single-cell transcriptome analysis. *Tas1r3* knockdown in Leydig cells was confirmed to impair both PKA/CREB signaling and the testosterone synthesis. Collectively, the findings of our study demonstrated that TAS1R3 deficiency negatively affects male reproductive performance by disrupting the testosterone synthesis pathway and influencing sperm quality and testicular histology.

The testes are complex endocrine glands that contain different cell types, such as germ cells that differentiate into mature spermatozoa and testosterone-producing Leydig cells. For adequate sperm quality, appropriate endocrine function of the testes is important, and many recent studies have implicated genetic factors in testicular endocrine function [35]. In this study, we proposed that *Tas1r3* can serve as an important genetic factor in male reproduction by influencing testosterone synthesis, affecting male reproductive performance, including sperm motility and testicular histology. Previous studies suggested that an appropriate testosterone level is crucial for normal sperm motility [36–38]. Testosterone activates ARs, which induce rapid influx of calcium through calcium channels, a process that is crucial for sperm motility and fertilization [39]. Consequently, reduced testosterone levels are strongly linked to decreased sperm motility. Furthermore, diminished intratesticular testosterone signaling disrupts three crucial testicular processes: blood-testis barrier (BTB) maintenance, premature release of round spermatids during differentiation, and the inability to release mature spermatozoa, leading to germ cell phagocytosis by Sertoli cells [40–42]. We confirmed that *Tas1r3* KO mice showed deteriorated sperm motility and velocity, particularly at 0 and 6 h after sperm collection, and lower testosterone levels, resulting in a lower fertilization rate and litter size. Previous studies analyzing the time course of fertilization of murine model reported that the majority of eggs retrieved from the ampulla 7 h post-mating formed 2-cell embryos, rendering our data at 0 and 6 h after sperm collection meaningful [43]. In addition, considering the evaluations of sperm motility, velocity, and defects in this study, it is reasonable to infer that *Tas1r3* plays a pivotal role in both the sperm elongation phase and development of motility during spermatogenesis. Histological analysis showed that testicular seminiferous tubules were significantly damaged in *Tas1r3* KO mice, suggesting that TAS1R3 is involved in testicular structure formation.

PKA signaling, a well-known molecular switch that can increase or decrease the activity of other proteins, was downregulated in *Tas1r3*-deficient testes. PKA is found in most cells and is considered a major target and effector of cAMP in multiple cellular signaling pathways [44,45]. Considering that TAS1R3 is a GPCR, which commonly regulates cAMP production by targeting adenylate cyclase [46,47], it is plausible to speculate that *Tas1r3* deficiency affects PKA activity within the testes. Our observations revealed that *Tas1r3*

deficiency decreased PKA signaling pathway activity in both testicular tissues and Leydig cells.

PKA signaling activates CREB, a ubiquitous nuclear transcription factor [48]. CREB attaches to the cAMP-response element, which contains a palindromic sequence and is present in various gene promoters [49]. In the testes, testosterone synthesis depends on PKA/CREB signaling-mediated regulation of steroidogenic enzymes [50–54]. In particular, CREB is a key regulator of promoter activation of *Star*, which regulates the rate-limiting phase of steroidogenesis, including testosterone biosynthesis [52]. Furthermore, the upstream region of the *Cyp11a1* gene, which catalyzes the initial step of steroidogenesis where the conversion of cholesterol into pregnenolone occurs, also has a CREB binding site in the promoter, allowing CREB to activate its promoter [55]. In the present study, *Tas1r3*-deficient mice showed significantly decreased testicular expression of *Creb1* and CREB-mediated key steroidogenic genes, *Star* and *Cyp11a1*, in contrast to the expression observed in WT mice [56,57]. Our results from transcriptomic analyses also confirmed that *Cyp17a1*, *Hsd3b1*, and *Hsd3b6*, other genes involved in testosterone biosynthesis, exhibited significantly decreased expression. In addition, circulating testosterone levels were significantly lower in *Tas1r3* KO mice. Thus, our findings suggest that testicular TAS1R3 plays a crucial role in male reproduction by regulating testosterone biosynthesis via the PKA/CREB/STAR signaling pathway and is required for adequate reproductive performance.

Leydig cells are a major producer of testosterone and act as key mediators in regulating spermatogenesis from early life to adulthood [14]. Testosterone and other androgens produced by FLCs during early life are necessary for the masculinization of the fetal embryo, which includes the differentiation of the mesonephric ducts, development of the male genital tract, gonadogenesis, and the formation of the ALC precursors [17,58]. Moreover, pubertal activation and the resulting secretion of testosterone by ALCs are crucial for initiating and sustaining spermatogenesis, in addition to the enhancement of male secondary sexual characteristics [59]. Herein, we found that *Tas1r3* is most abundant in Leydig cells than in other testicular cell types. Another novel aspect uncovered in this study is that knockdown of *Tas1r3* regulates the expression of steroidogenic enzymes in Leydig cells via the PKA/CREB/STAR signaling pathway, suggesting that nutritional signals can directly prompt Leydig cells to secrete testosterone via nutrient-sensing TAS1R3, irrespective of the negative feedback cycle of the hypothalamic–pituitary axis. Therefore, our findings provide a better understanding of regulation of gene expression during testosterone synthesis in Leydig cells and male infertility caused by Leydig cell dysfunction.

The nature of the ligands of TAS1R3 in the testes has yet to be established. In this study, we demonstrated that PKA signaling, a critical player in governing cellular metabolism and essential for the maintenance of energy homeostasis [60], was downregulated within the testicular context of *Tas1r3* KO mice. TAS1R3 functions as a nutrient-sensing receptor, and, similar to other organs, optimal functioning of the testes relies on vital nutrient-sensing signaling pathways [61]. Furthermore, considering that *Tas1r3* is also expressed in sperms, and L-glutamate, a physiological ligand of TAS1R3, is present in the female reproductive tract, the TAS1R3-ligand interaction is deemed essential in the entire process of male reproductive physiology [31].

In conclusion, the results of the present study demonstrate that TAS1R3 is a key regulator of male reproduction, particularly testosterone biosynthesis, via PKA/CREB/STAR signaling. To the best of our knowledge, this study is the first to suggest that TAS1R3 plays a crucial role in steroidogenesis and to clarify the mechanism by which TAS1R3 influences male reproduction via *in vivo* and *in vitro* knockout/knockdown models. These findings suggest that TAS1R3, a GPCR, an important target for various drugs, has potential as a novel therapeutic target [62] and provides new insights into male infertility-coping strategies.

3.1. Limitations of the study

Our study has a few limitations. First, the current conclusion regarding the role of TAS1R3 in male reproduction is based solely on the utilization of a murine cell line and an animal model, lacking support from clinical experiments. Despite the genetic similarities, additional human studies are required to demonstrate clinical relevance and determine the specific connection between male reproductive parameters and the expression of TAS1R3 in human testes. Second, we only focused on reproductive phenotypes of adult *Tas1r3* KO mice. A previous research has highlighted the essential role of the interaction between FLCs and testosterone in shaping the normal reproductive function in adulthood [63]. Finally, low fetal testosterone exposure during early life can affect the function and population of Leydig cells in adult testes [64]. Further study is needed to establish the involvement of TAS1R3 during early reproductive development within FLCs.

4. Materials and methods

4.1. Mice

B6; 129-Tas1r3tm1Csz/J (JAX 013066) mice were purchased from the Jackson Laboratory (West Grove, PA, USA). Exons 1–5 of *Tas1r3*, encoding the N-terminal extracellular domain, were replaced by a PGK-neomycin resistance cassette in (129 × 1/SvJ × 129S1/Sv)F1-*Kitl*⁺-derived R1 embryonic stem cells to generate the knockout of *Tas1r3* [22]. This strain was backcrossed to C57BL/6 for two generations by the donating laboratory. *Tas1r3* KO mice were crossbred with WT C57BL/6 mice for at least seven generations. For generation of WT and *Tas1r3* KO littermates, we adopted a breeding strategy involving the pairing of heterozygous individuals (*Tas1r3*^{+/-} × *Tas1r3*^{+/-}). Standard PCR was used to confirm the genotypes of the mice. Mice of both genotypes, matched for age and weight, were accommodated in a specific pathogen-free animal facility, maintaining constant humidity (55–60 %) and temperature (23 ± 2 °C) conditions. Standard pelleted chow and plain water were provided *ad libitum*. The body weight of each mouse and the amount of food and liquids consumed were measured weekly. All animal procedures were approved by the Institutional Animal Care and Use Committee of the Seoul National University (approval number: SNU-181001-2; Seoul, Korea).

4.2. Fertility assays

Mating of 10-week-old mice was used to measure reproductive capacity. WT males and females (six mating pairs and 51 offspring), WT males and *Tas1r3* KO females (three mating pairs and 24 offspring), *Tas1r3* KO males and WT females (six mating pairs and 27 offspring), and WT males and *Tas1r3* KO females (six mating pairs and 29 offspring) were analyzed. The vaginal plugs of the female mice and the number of pups produced were checked every morning.

4.3. Sperm analyses

Sperm suspensions obtained from mice were promptly placed into Petri dishes each containing a single droplet (300 μ L) of M2 media (non-capacitation media), covered with preheated paraffin oil, and finely minced. The incubation was carried out at 37 °C with 5 % CO₂. Following 15 min of incubation, the sperms were harvested.

After dilution and subjecting to heat exposure for immobilization, the concentration of sperm was determined using a Neubauer hemacytometer. Sperm samples were applied to glass microscope slides and allowed to air-dry for subsequent microscopic observation. For Coomassie blue staining, the sperm slides were incubated with a Coomassie brilliant blue 0.22 % solution for 2 min. The status of acrosome reaction in sperm was assessed by scoring 150 spermatozoa and calculating the ratio of spermatozoa exhibiting acrosome reaction. Computer-assisted sperm analysis (CASA) system (Hamilton Thorne Research, Beverly, MA, USA) was used to analyze various motility parameters, including velocity and the trajectory of motile movement in sperm samples, after 0, 6, and 18 h of incubation at 37 °C with 5 % CO₂. The proportions of sperm displaying motility and progressive motility, along with sperm motion variables, including VSL, VCL, and VAP, were assessed by the CASA system.

4.4. Histology

The entire testicular and epididymal tissues were isolated and fixed overnight in 10 % formalin before H&E staining, as previously described [65]. Tissues were processed and embedded in paraffin. Thick-sectioned tissues (5 μ m) were attached to a microscopic slide and stained with hematoxylin (Thermo Fisher Scientific, Waltham, MA, USA 6765007) and eosin (BBC Biochemical, Mount Vernon, WA, USA; 3610M1RA01) following standard procedures. Aperio ImageScope software v.12.3.3 (Leica Biosystems, Wetzlar, Germany) was used to capture the tissue sections.

4.5. Tissue preparation and total RNA extraction

The mice underwent overnight fasting (24 h) prior to euthanasia. Surgically removed testes and epididymides were promptly defatted after being placed in Petri dishes containing ice cold phosphate-buffered saline. The epididymal tissues were carefully segmented into the caput, corpus, and cauda regions. Rapidly frozen with liquid nitrogen, testicular and epididymal tissues were stored at -80 °C until further analyses. Frozen testicular and epididymal tissues were used for total RNA extraction, and the extracted RNA was purified using RNAqueous 4 PCR Kits (Ambion, Austin, TX, USA; AM1914) following the manufacturer's instructions. Prior to RNA sequencing, the quality and concentration of the extracted RNA were measured by a NanoDrop 2000 spectrophotometer (Thermo Fisher Scientific, Wilmington, DE, USA) and an Agilent 2100 Bioanalyzer (Agilent Technologies, Palo Alto, CA, USA). For RNA sequencing, samples with a RNA integrity number (RIN) exceeding 7.5 were selected.

4.6. Quantitative PCR with reverse transcription (qRT-PCR)

qRT-PCR was conducted as previously described [66]. Briefly, total RNA was extracted from the testicular tissues of mice and TM3 cells using RNAqueous (Cat# AM1914; Ambion) according to the manufacturer's instructions. The concentration of total RNA was confirmed using a NanoDrop 2000/2000c Spectrophotometer (Thermo Fisher Scientific). To synthesize cDNA (Cat# 11,917,010; Invitrogen), 1 μ g of RNA was used, and qRT-PCR was conducted using StepOnePlus (Real-time PCR System; Applied Biosystems, Foster City, CA, USA) and SYBRGreen (Cat# 4,367,659; Applied Biosystems). Relative quantification of gene expression was conducted using the 2^{- $\Delta\Delta$ Ct} method, and the mRNA expression level was normalized to that of *Gapdh*. Primers used for RT-qPCR are listed in Table S1.

4.7. RNA-sequencing (RNA-seq)

RNA-seq was conducted as previously described [67]. Initially, intact mRNA isolated from total RNA (1000 ng) was purified using the Dynabeads™ mRNA DIRECT™ Micro Purification kit (Cat# 61,021; Ambion). The ribosomal RNA was depleted using the RiboMinus™ Eukaryote System v2 (Cat# A15026; Life Technologies, Carlsbad, Canada). Next, cDNA transcriptome libraries were constructed using the Ion Total RNA Seq kit v2 (Cat# 4,475,936; Life Technologies), incorporating barcodes from the Ion Xpress RNA-Seq Barcode 01-16 kit (Cat# 4,475,485; Life Technologies). The whole-transcriptomic libraries were diluted to 100 pM and amplified using the Ion OneTouch™ 2 System and Ion PI Hi-Q OT2 200 kits (Cat# 4,474,779; Life Technologies). The template-positive ion-sphere particles were sequenced using the Ion PI Hi-Q Sequencing 200 kit (Cat# A26433; Life Technologies). These ion-sphere particles were loaded and incubated with polymerase on a chip from Ion PI Chip kit v3 (Cat# A26771; Life Technologies). RNA-seq was performed using an Ion Proton System (Life Technologies), and all experimental procedures were performed according to the manufacturer's instructions.

4.8. Bioinformatic analysis of RNA sequences

Raw RNA sequencing reads were quality controlled and adapter sequences were removed using the FASTQC tool, resulting in the generation of FASTAQ files. Sequencing reads were analyzed using Partek Flow® v7.0, 2018 (Partek, St. Louis, MO, USA). The reads were annotated to the Genome Reference Consortium Mouse Build 39 (mm39) using the STAR 2.5.3a aligner and quantification was performed using RefSeq transcript 93. DEGs were extracted using the R/Bioconductor package, DEseq2 (<http://bioconductor.org/>). Genes were considered DEGs if they showed an absolute fold change ≥ 1.5 and an adjusted *P*-value < 0.05 . A heatmap showing hierarchical clustering was generated using Genesis v1.8.1. The extracted DEGs were subjected to IPA using the IPA software (www.ingenuity.com) to investigate the enrichment of specific pathways among DEGs. Additionally, gene set enrichment analysis (GSEA) was performed to validate the IPA results. Our RNA-seq data were submitted to the GEO (accession number: GSE226995).

4.9. Preparation of protein and western blotting

Testicular tissues isolated from mice were lysed by adding 1 mL of Tissue Extraction Reagent 1 (Cat# FNN0071; Invitrogen) with 10 μ l protease inhibitor cocktail solution (Cat# P2714; Sigma-Aldrich, St. Louis, MO, USA), followed by homogenization. Similarly, protein was extracted from TM3 cells using radio-immunoprecipitation assay cell lysis and extraction buffer. The concentration of extracted protein was confirmed using the Pierce BCA Protein Assay Kit (Cat# 23,227; Thermo Fisher Scientific). For electrophoresis, each protein lysate (20 μ g) was subjected to sodium dodecyl sulfate-polyacrylamide gels. Transfer to polyvinylidene fluoride membranes were performed subsequently. The membranes were blocked with 5 % non-fat milk for 1 h at room temperature and incubated with primary antibodies, goat *anti-TAS1R3* (1:300) (Cat# ABIN571574; antibodies-online GmbH, Aachen, Germany), monoclonal rabbit *anti-CREB* (1:500) (Cat# ab32515; Abcam, Cambridge, UK), and monoclonal rabbit *anti-phospho-CREB* (1:1000) (Cat# 9198 S; Cell Signaling Technology, Danvers, MA, USA). Monoclonal mouse *anti- α -tubulin* (1:10,000) antibodies (Cat #T5168; Sigma-Aldrich) were used as control. The membranes were washed three times with TBS-T for 10 min, then incubated with secondary antibodies, horseradish peroxidase-conjugated rabbit anti-goat secondary antibodies (1:1000) (Cat# SA007; GenDEPOT, Baker, TX, USA), goat anti-rabbit secondary antibodies (1:5000) (Cat# 7074 S; Cell Signaling Technology), and goat anti-mouse secondary antibodies (1:10,000) (Cat# G21040; Invitrogen). After washing the membrane three times with TBS-T for 10 min, bands were visualized using enhanced chemiluminescence Western blot detection reagents (Cat# RPN2209; Cytiva, Marlborough, MA, USA).

4.10. Enzyme-linked immunosorbent assay (ELISA)

ELISA kits designed for mouse testosterone (Cat# ab285350; Abcam) were employed to measure the concentrations of testosterone in serum and urine samples from mice, as well as in cell-conditioned media, following the manufacturer's instructions.

4.11. Cell culture and transfection

Murine TM3 cells (Cat# CRL-1714; American Type Culture Collection, Manassas, VA, USA) were cultured at 37 °C with 5 % CO₂ in Dulbecco's modified Eagle's medium/F-12 (Cat# LM002-04; WelGENE Inc., Daegu, Korea), with 10 % fetal bovine serum and 1 % penicillin-streptomycin solution added. For knocking down *Tas1r3*, 1×10^5 TM³ cells per well were seeded in a 6-well culture plate approximately 24 h before transfection. Upon reaching 60 % confluency, each well was transfected with *Tas1r3* siRNA (20 nM; Bioneer, Daejeon, South Korea) and Lipofectamine™ RNAiMAX® complexes (Invitrogen, Thermo Fisher Scientific, USA) according to the manufacturer's instructions. Following 48 h incubation, all media were collected, and the cells were harvested for subsequent biochemical analysis. The siRNAs' target sequences utilized for the knockdown are detailed in [Table S2](#).

4.12. Bioinformatics data analyses of public database

Transcriptome studies on mouse testes were searched on the GEO database using the keywords "testis" and "single-cell RNA-seq." The inclusion criteria for the dataset involved expression profiling using single-cell RNA sequencing method, with samples originating exclusively from mouse testes. Our analysis was conducted on a dataset with the GEO series accession number GSE190043. The expression pattern of TAS1R3 specific to cell types in the mouse testicular tissues was extracted for statistical analysis. UMAP construction, cell type identification, and transcript profiling analysis were conducted by the R software "Seurat package", following the previously outlined methodology [68]. Cell type annotations were assigned to corresponding clusters using markers specific to each cell type, as previously described [69].

4.13. Statistical analysis

The mean values of two groups were compared using Student's *t*-test, and the means of multiple experimental groups were statistically analyzed using one-way analysis of variance, followed by Tukey's multiple comparison tests. All data are presented as mean \pm SEM. *P* < 0.05 was considered statistically significant. GraphPad Prism 9.3.0 for Windows (GraphPad Software, San Diego, CA, USA), Partek Flow® v7.0 (Partek), and IPA (www.ingenuity.com) were used for statistical analyses.

Funding

This study was supported by a grant from the Rural Development Administration of Korea (grant number PJ017031).

Data availability statement

The raw transcriptome dataset generated during the current study is available in the GEO repository (accession numbers GSE226995). The data that support the findings of this study are available from the corresponding authors upon reasonable request.

CRediT authorship contribution statement

Woo-Jeong Shon: Writing – original draft, Supervision, Methodology, Investigation, Funding acquisition, Conceptualization. **Hobin Seong:** Writing – original draft, Methodology, Investigation, Conceptualization. **Jaе Won Song:** Writing – original draft, Methodology, Investigation, Conceptualization. **Dong-Mi Shin:** Funding acquisition.

Declaration of competing interest

The authors declare the following financial interests/personal relationships which may be considered as potential competing interests: Woo-Jeong Shon reports financial support was provided by Rural Development Administration of Republic of Korea.

Acknowledgments

Not applicable.

Appendix A. Supplementary data

Supplementary data to this article can be found online at <https://doi.org/10.1016/j.heliyon.2024.e24577>.

References

- [1] F. Zegers-Hochschild, et al., The international glossary on infertility and fertility care, *Hum. Reprod.* 32 (9) (2017) 1786–1801, 2017.
- [2] M. Vander Borgh, C. Wyns, Fertility and infertility: definition and epidemiology, *Clin. Biochem.* 62 (2018) 2–10.
- [3] R. Nosrati, et al., Microfluidics for sperm analysis and selection, *Nat. Rev. Urol.* 14 (12) (2017) 707–730.
- [4] A. Agarwal, et al., Male infertility, *Lancet* 397 (10271) (2021) 319–333.
- [5] S. Sabra, M.S. Al-Harbi, An influential relationship of seminal fluid microbial infections and infertility, Taif Region, KSA. *World J Med Sci* 10 (1) (2014) 32–37.
- [6] R. Qu, et al., ADGB variants cause asthenozoospermia and male infertility, *Hum. Genet.* 142 (6) (2023) 735–748.
- [7] Y. Chang, et al., Molecular genetic mechanisms of teratozoospermia, *Zygote* 31 (2) (2023) 101–110.
- [8] H. Levine, et al., Temporal trends in sperm count: a systematic review and meta-regression analysis of samples collected globally in the 20th and 21st centuries, *Hum. Reprod. Update* 29 (2) (2023) 157–176.
- [9] K.P. Li, X.S. Yang, T. Wu, The effect of antioxidants on sperm quality parameters and pregnancy rates for idiopathic male infertility: a network meta-analysis of randomized controlled trials, *Front. Endocrinol.* 13 (2022) 810242.
- [10] C.W. Bak, et al., Hormonal imbalances and psychological scars left behind in infertile men, *J. Androl.* 33 (2) (2012) 181–189.
- [11] Y. Frederiksen, et al., Efficacy of psychosocial interventions for psychological and pregnancy outcomes in infertile women and men: a systematic review and meta-analysis, *BMJ Open* 5 (1) (2015) e006592.
- [12] A.K. Wu, et al., Time costs of fertility care: the hidden hardship of building a family, *Fertil. Steril.* 99 (7) (2013) 2025–2030.
- [13] W.D. Petok, Infertility counseling (or the lack thereof) of the forgotten male partner, *Fertil. Steril.* 104 (2) (2015) 260–266.
- [14] B.R. Zirkkin, V. Papadopoulos, Leydig cells: formation, function, and regulation, *Biol. Reprod.* 99 (1) (2018) 101–111.
- [15] Y. Shima, Development of fetal and adult Leydig cells, *Reprod. Med. Biol.* 18 (4) (2019) 323–330.
- [16] I. Bhattacharya, S. Dey, Emerging concepts on Leydig cell development in fetal and adult testis, *Front. Endocrinol.* 13 (2023).
- [17] S.J. Potter, D.L. Kumar, T. DeFalco, Origin and differentiation of androgen-producing cells in the gonads, *Results Probl. Cell Differ.* 58 (2016) 101–134.
- [18] F.M. Kohn, Testosterone and body functions, *Aging Male* 9 (4) (2006) 183–188.
- [19] W. Zhao, et al., Circulating sex hormone levels in relation to male sperm quality, *BMC Urol.* 20 (1) (2020) 101.
- [20] R. Luboshitzky, et al., Seminal plasma androgen/oestrogen balance in infertile men, *Int. J. Androl.* 25 (6) (2002) 345–351.
- [21] K. Sanematsu, et al., Structure, function, and signaling of taste G-protein-coupled receptors, *Curr. Pharmaceut. Biotechnol.* 15 (10) (2014) 951–961.
- [22] G.Q. Zhao, et al., The receptors for mammalian sweet and umami taste, *Cell* 115 (3) (2003) 255–266.
- [23] S.V. Wu, et al., Expression of bitter taste receptors of the T2R family in the gastrointestinal tract and enteroendocrine STC-1 cells, *Proc. Natl. Acad. Sci. USA* 99 (4) (2002) 2392–2397.
- [24] B.R. Simon, et al., Sweet taste receptor deficient mice have decreased adiposity and increased bone mass, *PLoS One* 9 (1) (2014) e86454.
- [25] V.O. Murovets, E.A. Sozontov, T.G. Zacheplilo, The effect of the taste receptor protein T1R3 on the development of islet tissue of the murine pancreas, *Dokl. Biol. Sci.* 484 (1) (2019) 1–4.
- [26] B. Martin, et al., Altered learning, memory, and social behavior in type 1 taste receptor subunit 3 knock-out mice are associated with neuronal dysfunction, *J. Biol. Chem.* 292 (27) (2017) 11508–11530.
- [27] A. Gustavsson, et al., Cost of disorders of the brain in Europe 2010, *Eur. Neuropsychopharmacol.* 21 (10) (2011) 718–779.
- [28] B. Mosinger, et al., Genetic loss or pharmacological blockade of testes-expressed taste genes causes male sterility, *Proc. Natl. Acad. Sci. USA* 110 (30) (2013) 12319–12324.
- [29] T. Gong, et al., Longitudinal expression of testicular TAS1R3 from prepuberty to sexual maturity in congjiang Xiang pigs, *Animals : an open access journal from MDPI* 11 (2) (2021) 437.

- [30] T. Gong, et al., Expression patterns of taste receptor type 1 subunit 3 and α -gustducin in the mouse testis during development, *Acta Histochem.* 118 (1) (2016) 20–30.
- [31] M. Frolíkova, et al., The role of taste receptor mTAS1R3 in chemical communication of gametes, *Int. J. Mol. Sci.* 21 (7) (2020) 2651.
- [32] A. Sironen, et al., Sperm defects in primary ciliary dyskinesia and related causes of male infertility, *Cell. Mol. Life Sci.* 77 (11) (2020) 2029–2048.
- [33] S.L. Cafe, A.L. Anderson, B. Nixon, In vitro induction and detection of acrosomal exocytosis in human spermatozoa, *Bio Protoc* 10 (14) (2020) e3689.
- [34] J. Buñay, et al., A decrease of docosahexaenoic acid in testes of mice fed a high-fat diet is associated with impaired sperm acrosome reaction and fertility, *Asian J. Androl.* 23 (3) (2021) 306–313.
- [35] S. Basaria, Male hypogonadism, *Lancet* 383 (9924) (2014) 1250–1263.
- [36] A.J. Ridley, L. Blasco, Testosterone and gossypol effects on human sperm motility, *Fertil. Steril.* 36 (5) (1981) 638–642.
- [37] J.D. Meeker, L. Godfrey-Bailey, R. Hauser, Relationships between serum hormone levels and semen quality among men from an infertility clinic, *J. Androl.* 28 (3) (2007) 397–406.
- [38] M.Z. Keskin, et al., The relationship between serum hormone levels (follicle-stimulating hormone, luteinizing hormone, total testosterone) and semen parameters, *Arch. Ital. Urol. Androl.* 87 (3) (2015) 194–197.
- [39] I. Thanaboonyawat, et al., Application of testosterone supplementation in semen to improve sperm motility in asthenozoospermic males, *Arch. Gynecol. Obstet.* 296 (3) (2017) 589–596.
- [40] W.H. Walker, Androgen actions in the testis and the regulation of spermatogenesis, in: C.Y. Cheng, F. Sun (Eds.), *Molecular Mechanisms in Spermatogenesis*, Springer International Publishing, Cham, 2021, pp. 175–203.
- [41] H.H. Yan, et al., Blood-testis barrier dynamics are regulated by testosterone and cytokines via their differential effects on the kinetics of protein endocytosis and recycling in Sertoli cells, *Faseb. J.* 22 (6) (2008) 1945–1959.
- [42] L. O'Donnell, et al., Testosterone withdrawal promotes stage-specific detachment of round spermatids from the rat seminiferous epithelium, *Biol. Reprod.* 55 (4) (1996) 895–901.
- [43] F.A. La Spina, et al., Mouse sperm begin to undergo acrosomal exocytosis in the upper isthmus of the oviduct, *Dev. Biol.* 411 2 (2016) 172–182.
- [44] H. Zhang, et al., Complex roles of cAMP–PKA–CREB signaling in cancer, *Exp. Hematol. Oncol.* 9 (1) (2020) 32.
- [45] A. Koschinski, M. Zaccolo, Activation of PKA in cell requires higher concentration of cAMP than in vitro: implications for compartmentalization of cAMP signalling, *Sci. Rep.* 7 (1) (2017) 14090.
- [46] S.J. Lee, I. Depoortere, H. Hatt, Therapeutic potential of ectopic olfactory and taste receptors, *Nat. Rev. Drug Discov.* 18 (2) (2019) 116–138.
- [47] F. Li, Taste perception: from the tongue to the testis, *Mol. Hum. Reprod.* 19 (6) (2013) 349–360.
- [48] A.J. Shaywitz, M.E. Greenberg, CREB: a stimulus-induced transcription factor activated by a diverse array of extracellular signals, *Annu. Rev. Biochem.* 68 (1999) 821–861.
- [49] S. Kumar, et al., The expression of CKLF2B is regulated by GATA1 and CREB in the Leydig cells, which modulates testicular steroidogenesis, *Biochimica et Biophysica Acta (BBA) - Gene Regulatory Mechanisms* 1861 (12) (2018) 1063–1075.
- [50] A.H. Payne, M.P. Hardy, SpringerLink, The Leydig cell in health and disease, in: *Contemporary Endocrinology*, Humana Press, Totowa, N.J., 2007, pp. 157–171.
- [51] Y. Nakayama, et al., Cysteine sulfoxides enhance steroid hormone production via activation of the protein kinase A pathway in testis-derived I-10 tumor cells, *Molecules* 25 (20) (2020).
- [52] P.R. Manna, et al., Transcriptional regulation of the mouse steroidogenic acute regulatory protein gene by the cAMP response-element binding protein and steroidogenic factor 1, *J. Mol. Endocrinol.* 30 (3) (2003) 381–397.
- [53] F. Oury, et al., Endocrine regulation of male fertility by the skeleton, *Cell* 144 (5) (2011) 796–809.
- [54] A. Tan, et al., Expression patterns of C1ql4 and its cell-adhesion GPCR Bai3 in the murine testis and functional roles in steroidogenesis, *Faseb. J.* 33 (4) (2019) 4893–4906.
- [55] B.-c. Chung, I.-C. Guo, S.-J. Chou, Transcriptional regulation of the CYP11A1 and ferredoxin genes, *Steroids* 62 (1) (1997) 37–42.
- [56] P.R. Manna, et al., Role of the steroidogenic acute regulatory protein in health and disease, *Endocrine* 51 (1) (2016) 7–21.
- [57] S.R. King, H.A. LaVoie, Gonadal transactivation of STARD1, CYP11A1 and HSD3B, *FBL* 17 (3) (2012) 824–846.
- [58] Q. Wen, C.Y. Cheng, Y.-X. Liu, Development, function and fate of fetal Leydig cells, *Semin. Cell Dev. Biol.* 59 (2016) 89–98.
- [59] H. Chen, et al., Leydig cell stem cells: identification, proliferation and differentiation, *Mol. Cell. Endocrinol.* 445 (2017) 65–73.
- [60] E. London, C.A. Stratakis, The regulation of PKA signaling in obesity and in the maintenance of metabolic health, *Pharmacol. Ther.* 237 (2022) 108113.
- [61] J. Dupont, et al., Nutritional signals and reproduction, *Mol. Cell. Endocrinol.* 382 (1) (2014) 527–537.
- [62] K. Sriram, P.A. Insel, G protein-coupled receptors as targets for approved drugs: how many targets and how many drugs? *Mol. Pharmacol.* 93 (4) (2018) 251–258.
- [63] T. Defalco, et al., Testosterone levels influence mouse fetal Leydig cell progenitors through notch signaling, *Biol. Reprod.* 88 (4) (2013) 91.
- [64] K.R. Kilcoyne, et al., Fetal programming of adult Leydig cell function by androgenic effects on stem/progenitor cells, *Proc. Natl. Acad. Sci. U. S. A.* 111 (18) (2014) E1924–E1932.
- [65] C. Li, et al., AGRP neurons modulate fasting-induced anxiolytic effects, *Transl. Psychiatry* 9 (1) (2019) 111.
- [66] W.J. Shon, et al., Renal transcriptome profiles in mice reveal the need for sufficient water intake irrespective of the drinking water type, *Sci. Rep.* 12 (1) (2022) 10911.
- [67] B.R. Simon, et al., Sweet taste receptor deficient mice have decreased adiposity and increased bone mass, *PLoS One* 9 (1) (2014).
- [68] Y. Hao, et al., Integrated analysis of multimodal single-cell data, *Cell* 184 (13) (2021), 3573–3587.e29.
- [69] S. Lukassen, et al., Characterization of germ cell differentiation in the male mouse through single-cell RNA sequencing, *Sci. Rep.* 8 (2018).